Synthetic and Systems Biotechnology 9 (2024) 144–151

Contents lists available at ScienceDirect

Synthetic and Systems Biotechnology

journal homepage: www.keaipublishing.com/en/journals/synthetic-and-systems-biotechnology

Original Research Article

Identification of crucial roles of transcription factor IhfA on high production of free fatty acids in *Escherichia coli*

Lixia Fang [a,b,1], Ziyi Han [a,b,1], Xueru Feng [a,b], Xueyan Hao [a,b], Mengxiao Liu [a,b], Hao Song [a,b], Yingxiu Cao [a,b,*]

[a] Frontiers Science Center for Synthetic Biology and Key Laboratory of Systems Bioengineering (Ministry of Education), School of Chemical Engineering and Technology, Tianjin University, Tianjin, 300072, China
[b] Frontiers Research Institute for Synthetic Biology, Tianjin University, China

ARTICLE INFO

Keywords:
Free fatty acids
CRISPRi
ihfA
Cell membrane
ROS

ABSTRACT

Transcription factor engineering has unique advantages in improving the performance of microbial cell factories due to the global regulation of gene transcription. Omics analyses and reverse engineering enable learning and subsequent incorporation of novel design strategies for further engineering. Here, we identify the role of the global regulator IhfA for overproduction of free fatty acids (FFAs) using CRISPRi-facilitated reverse engineering and cellular physiological characterization. From the differentially expressed genes in the *ihfA*$^{L-}$ strain, a total of 14 beneficial targets that enhance FFAs production by above 20 % are identified, which involve membrane function, oxidative stress, and others. For membrane-related genes, the engineered strains obtain lower cell surface hydrophobicity and increased average length of membrane lipid tails. For oxidative stress-related genes, the engineered strains present decreased reactive oxygen species (ROS) levels. These gene modulations enhance cellular robustness and save cellular resources, contributing to FFAs production. This study provides novel targets and strategies for engineering microbial cell factories with improved FFAs bioproduction.

1. Introduction

Free fatty acids (FFAs) are essential precursors for the synthesis of alkanes, fatty alcohols, fatty acid alkyl esters, and other fatty acid-derived chemicals (FACs), which have wide applications in biofuels, pharmaceuticals, feed additives, and others [1,2]. In recent years, FFAs production via metabolically engineered microbes has become a green and promising alternative to conventional extraction methods based on petroleum or plant biomass [3,4]. In microbial cells, fatty acid metabolism involves the interactions of multiple reactions and intermediates [2,5,6], which are subject to complicated metabolic networks. Thus, it is highly desirable to identify useful gene targets that can be re-engineered for enhanced FFAs biosynthesis.

In *Escherichia coli*, FFAs biosynthesis has been frequently enhanced by rational metabolic engineering [7–9]. Therein, key enzymes in the FFAs biosynthetic pathways, such as the truncated fatty acyl-ACP thioesterase TesA, and key genes in the degradation pathways, such as *fadD* or *fadE*, were applied for combinatorial optimization to improve FFAs production [8,9]. However, these strategies are mainly focused on the engineering of FFAs metabolic pathway itself, and further strengthening FFAs production is hindered by the limited understanding of the highly complex cellular interaction networks [10]. In recent years, transcription factor engineering has been applied to the optimization of microbial cell factories, which makes the metabolic regulation carried out at a systematic or global level [11]. In *E. coli*, FadR functions as an activator of *fabA* and *fabB* as well as a repressor of the β-oxidation (*fad*) regulon [12], while FabR acts as a repressor for the *fabA* and *fabB* genes [13]. As expected, the transcription factors FadR and FabR have been engineered to redirect the fluxes toward FFAs production [14,15]. However, to the best of our knowledge, few works on additional transcription factors have been reported to further elucidate and improve FFAs biosynthesis.

Integration host factor (IHF) is known originally as a cofactor in the site-specific recombination of bacteriophage lambda [16]. Indeed, IHF can influence global transcription through its ability to bind and bend

Peer review under responsibility of KeAi Communications Co., Ltd.
* Corresponding author. Frontiers Science Center for Synthetic Biology and Key Laboratory of Systems Bioengineering (Ministry of Education), School of Chemical Engineering and Technology, Tianjin University, Tianjin, 300072, China.
E-mail address: caoyingxiu@tju.edu.cn (Y. Cao).
[1] The authors contribute equally.

https://doi.org/10.1016/j.synbio.2024.01.007
Received 19 October 2023; Received in revised form 7 January 2024; Accepted 18 January 2024
Available online 26 January 2024

DNA [17]. In *E. coli*, IHF is composed of an α-subunit and β-subunit encoded by the *ihfA* and *ihfB* genes, respectively. IhfA has been verified as a global dual transcriptional regulator on amino acid metabolism [18]. In our previous study, the influence of *ihfA* knockdown on FFAs biosynthesis was reported, and the transcriptomic and proteomic analyses showed that *ihfA* knockdown significantly modulated the expression of hundreds of genes ($ihfA^{L-}$ vs. Control) [7]. Through cross-analysis, some targets were found to enhance fatty acid synthesis. However, the mechanism of *ihfA* perturbation on fatty acid synthesis still needs to be improved and deepened. In recent years, CRISPRi has been widely used to down-regulate gene expression due to its ease of design and manipulation, which is an important method to dissect the mechanism and modify metabolic networks [19–21].

In this study, the role of the global regulator IhfA for FFAs overproduction was identified using CRISPRi-facilitated reverse engineering and cellular physiological characterization. First, 14 beneficial CRISPRi targets (*pspA*, *rpsK*, *ompX*, *dps*, *iadA*, *gatY*, *sodB*, *sra*, *rbsB*, *gltI*, *pspD*, *yhcN*, *yegU*, *phoA*) were identified from the differentially expressed genes at the transcript and protein levels in the $ihfA^{L-}$ strain compared to the Control strain. Then, lower cell surface hydrophobicity, increased average length of membrane lipid tails and decreased reactive oxygen species (ROS) level were obtained in the engineered strains targeting membrane-related genes and oxidative stress-related genes, respectively. We speculate that these perturbations contribute to enhancing cellular robustness, meanwhile inhibiting protein expression in favor of saving cellular resources for FFAs biosynthesis. Our results provide new targets and novel strategies for the engineering of FFAs bioproduction.

2. Materials and methods

2.1. Experimental materials

All genes, plasmids, and strains utilized in this study are listed in Tables S1, S2, and S3, respectively. *E. coli* Trans1-T1 was utilized for general cloning. *E. coli* BL21(DE3) derived strains were utilized for fermentation. Target site complementary sequences of sgRNAs were designed by a user-friendly web tool (http://crispor.org) [22]. The designed primers were annealed and target site complementary sequences were ligated into plasmid Sg–S by Golden Gate assembly [23,24], allowing the construction of plasmids for expression of sgRNAs targeting any expected genomic locus. Primers utilized to construct the plasmids Sg-gene are listed in Table S4. The pCT plasmid was constructed by ligating the coding sequence of *tesA'* from the pCF plasmid into the pACYCDuet-1 digested by NdeI and KpnI. The sequences of *dps*, *sodB*, and *yhcN* were amplified from *E. coli* BL21(DE3) genomic DNA and then ligated into the Sg-BAD plasmid using NovoRec plus One step PCR Cloning Kit (Novoprotein, China), resulting in the plasmids Sg-BAD-dps, Sg-BAD-sodB, and Sg-BAD-yhcN, respectively. Primers utilized for amplifying the sequences of *dps*, *sodB* and *yhcN* are listed in Table S5.

2.2. Culturing conditions and media

The engineered strains were cultured at 30 °C and shaken at 220 rpm. Tube fermentation was performed in three biological replicates. Single colonies of each strain were inoculated into 2 mL LB medium. 1 % (V/V) of overnight cultures was re-inoculated into 5 mL of modified M9 medium in a glass tube. When OD_{600} reached about 1.0, the cultures were induced with 1 mM IPTG and allowed to grow for additional 40 h. Modified M9 medium [25] was as described: 3 g/L KH_2PO_4, 12.8 g/L $Na_2HPO_4{\cdot}7H_2O$, 0.5 g/L NaCl, 2 g/L yeast extract, 2 g/L NH_4Cl, 30 g/L glycerol, 11.1 mg/L $CaCl_2$, 0.25 g/L $MgSO_4{\cdot}7H_2O$, 10 mg/L thiamine, and 0.1 % (v/v) Triton X100. Additionally, 1 mL/L trace metal stock solution was supplemented, which contained 27 g/L $FeCl_3{\cdot}6H_2O$, 1.9 g/L, $CuSO_4{\cdot}5H_2O$, 2 g/L $ZnCl_2$, 2 g/L $Na_2MoO_4{\cdot}2H_2O$, and 0.5 g/L H_3BO_3. pH was adjusted to about 7.2 by Tris. If necessary, 100 mg/L ampicillin or 34 mg/L chloramphenicol was supplemented.

2.3. FFAs extraction and analysis

The extraction and quantification of FFAs were performed as described previously [7,26]. Specifically, 500 μL of cell culture was harvested, acidified with 50 μL of concentrated HCl, spiked with 100 μg of heptadecanoic acid as internal standard, and extracted twice with 500 μL of ethyl acetate. The extracted FFAs were determined using a SHIMADZU Nexis GC-2030 gas chromatograph equipped with a TG-WaxMS A column (length, 30 m; inner diameter, 0.32 mm; film, 0.25 μm; Thermo Scientific) and a barrier discharge ionization detector operating under a constant flow rate of the carrier gas (helium) at 1 mL/min. The temperature program was the following: hold at 50 °C for 2 min, then heat to 245 °C at 30 °C/min and hold for 23 min. Individual fatty acid species were determined by comparing the peak areas with that of the internal standard using the Labsolutions 5.98 software. Total FFAs concentrations were calculated as the sum of C12 to C18.

2.4. Membrane lipid composition

The membrane lipids were extracted by the Bligh and Dyer method with minor modifications [27,28]. Cells were harvested at the mid-logarithmic phase (12 h after IPTG induction), washed twice with cold sterile water, resuspended in 2 mL methanol, and sonicated for three 30 s bursts. Then, 1.4 mL of this processed solution was added with 20 μL of the solution containing 1 mg/mL heptadecanoic acid in methanol. These mixtures were incubated at 70 °C for 15 min and cooled to room temperature. After centrifuging at 4000 g for 5 min, the supernatant and pellet were processed separately. The pellet was added with 750 μL of chloroform, then vortexed for 5 min at 150 rpm and 37 °C. The supernatant was added with 1.4 mL of ultrapure water and transferred back to the chloroform-treated pellet. The mixture was vortexed for 2 min and centrifuged at 3000 g for 5 min. Then, the bottom layer was transferred to a new tube and evaporated to remove the solvent. The dried sample was added with 2 mL of 1 M HCl in methanol, heated at 80 °C for 30 min, and cooled to room temperature. The cold solution was added with 2 mL of aqueous NaCl (0.9 wt%) and 1 mL of hexane, vortexed for 2 min, and then centrifuged at 2000 g for 2 min.

The upper layer was analyzed by a SHIMADZU Nexis GC-2030 gas chromatograph equipped with a TG-5MS A column (length, 30 m; inner diameter, 0.32 mm; film, 0.25 μm; Thermo Scientific) and a Barrier Discharge Ionization Detector operating under a constant flow rate of the carrier gas (helium) at 1 mL/min. The temperature program was following: hold at 50 °C for 2 min, heat to 200 °C at 25 °C/min and hold for 1 min, then heat to 315 °C at 25 °C/min and hold for 2 min. Individual lipid species were determined by comparing the peak areas with that of the internal standard using the Labsolutions 5.98 software.

2.5. Cell surface hydrophobicity

Cell surface hydrophobicity was quantified following the previously described MATH method [28,29]. Cell cultures were harvested at the midlogarithmic phase (12 h after IPTG induction), followed by centrifugation at 5000 rpm for 10 min. Pellets were then washed twice and resuspended in PBS buffer at a final OD_{600} of 0.6 (OD1). Then, 1 mL of dodecane was added to 4 mL of cell suspension, and the mixture was vortexed at 2500 rpm for 10 min. The mixtures were left to settle for 15 min, and the OD_{600} of the aqueous phase (OD2) was measured. Cell surface hydrophobicity was calculated using the following equation: percent partitioning = (OD1-OD2)/OD1 × 100.

2.6. ROS measurement

The intracellular ROS level was assessed by using the reactive oxygen species assay kit (Solarbio). Briefly, samples were collected at 40 h after IPTG induction and washed twice with PBS buffer. The cells were then resuspended in 0.5 mL PBS buffer containing 10 μM oxidant-sensitive

probe 2,7-dichlorofluorescin diacetate (DCFH-DA), incubated at 30 °C for 30 min, and then washed twice with PBS buffer. The fluorescence of the sample was measured using a microplate reader (SpectraMax M2, Molecular Devices) with λ_{EX} 488 nm and λ_{EM} 525 nm or imaged using a fluorescence microscope (Olympus BX53).

2.7. qRT-PCR analysis

Samples were collected at 3 h after IPTG induction, and total RNA was extracted using the U-Fast Bacterial RNA Extraction kit (Beijing Zoman Biotechnology, China). Subsequently, cDNAs were synthesized using the Reverse Transcriptase Kit (Beijing Zoman Biotechnology, China). qRT-PCR reactions were performed following the instructions of 2x SYBR qPCR Mix (Beijing Zoman Biotechnology, China) in a Quantagene Q225 system. A list of the qRT-PCR primer is provided in Table S5. The expression levels for each gene in the engineered strain were calculated by normalizing to the 16S rRNA gene and relative to the Control strain using the ΔΔCT method [30,31].

2.8. Statistical analysis

Student's *t*-test was used to investigate the significance of differences between two groups. Calculation was conducted using Graphpad prism 9. Statistical significance was determined with *P* values defined as $^{*}P < 0.05$, $^{**}P < 0.005$, $^{***}P < 0.001$ for this experiment.

3. Results and discussions

3.1. Identification of beneficial genes enhancing FFAs production

The *ihfA*$^{L-}$ strain was constructed by expressing dCas9 and sgRNA targeting the non-template (NT) strand of the *ihfA* gene at the terminal

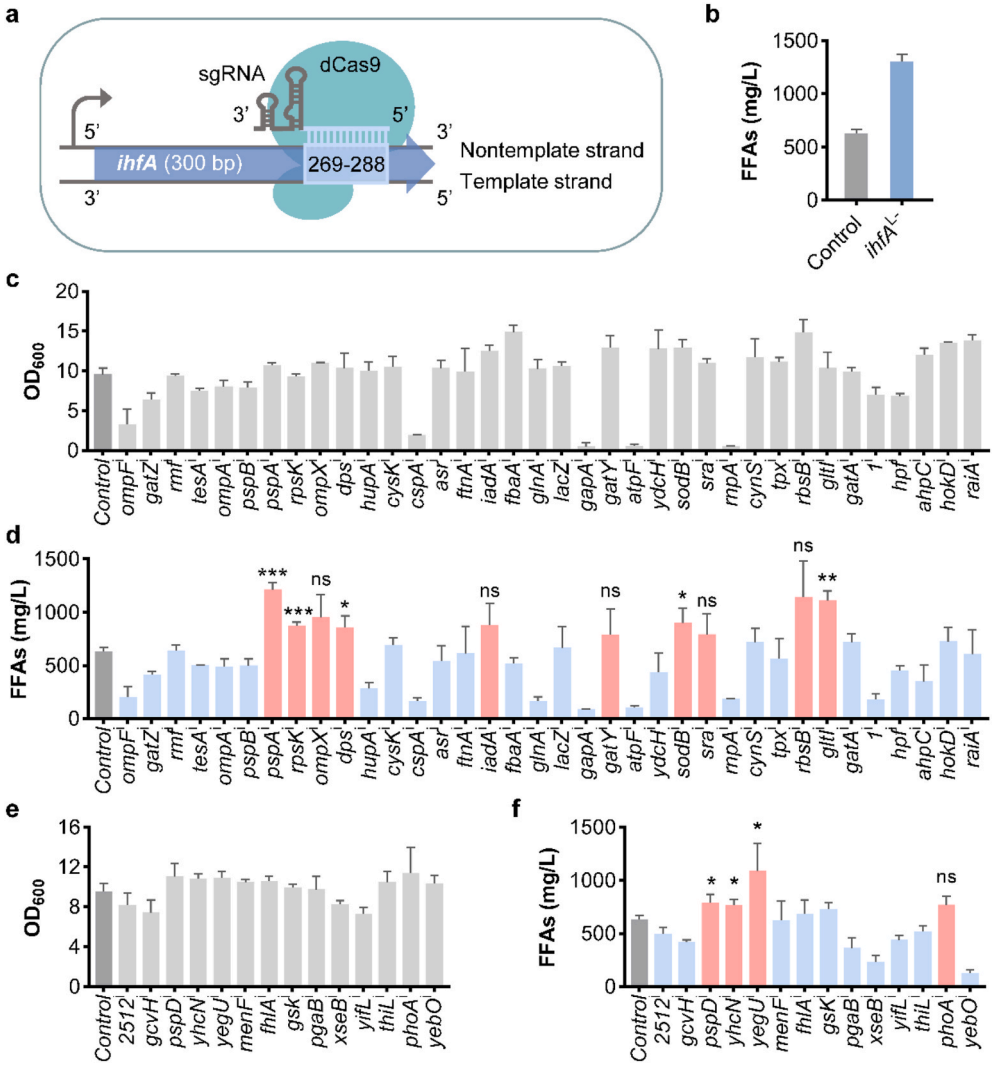

Fig. 1. Identification of beneficial genes enhancing FFAs production in the *ihfA*$^{L-}$ strain. (a) The *ihfA*$^{L-}$ strain expressing dCas9 and sgRNA binds the nontemplate strand of *ihfA* gene at the terminal region. (b) FFAs production in the *ihfA*$^{L-}$ and Control strains. (c) Cell growth of the engineered strains that repress genes selected from the comparative transcriptomic analysis of *ihfA*$^{L-}$ and Control. *lpp*, *fis*, *rplW*, *pal*, *pflB*, *tyrU*, *glpK*, *csrB*, and *adhE* have been engineered in our previous study [7]. *lysT* failed to design sgRNA. Repression of *rpmC*, *rplT*, *rbsD*, *rpsO*, *ptsH*, *rpmF*, *rpmI*, *yidD*, *rplQ*, *rplE*, *rpsB*, *rpsN*, *rplK*, *rpsD*, *rplF*, *rpsU*, *cydA*, *rpsM*, *secB*, *rpsG*, *folE*, *rplN*, *rpsS*, and *rpsF* destroyed cell growth completely. (d) FFAs production of the engineered strains that repress genes selected from the comparative transcriptomic analysis of *ihfA*$^{L-}$ and Control. (e) Growth of the engineered strains that repress genes selected from the comparative proteomic analysis of *ihfA*$^{L-}$ and Control. *norR*, *aroM*, *ihfA*, *waaF*, *nrdE*, *npr*, *yihU*, *sdhB*, *lpp*, *glpG*, *pal*, *cirA*, *ftsQ*, *secB*, *rplW*, *plsY*, *creC*, *yijO*, and *fis* have been examined in the above part or our previous study [7]. *insA-29* and *ecnB* failed to design sgRNAs. The *ssuD*, *ascG*, and *clpS* strains were unable to grow. *2512* represents the gene numbered ECD_02512 in BL21(DE3). (f) FFAs production of the engineered strains that repress genes selected from the comparative proteomic analysis of *ihfA*$^{L-}$ and Control. Error bars on graphs are presented as s.d.

region in our previous study [7](Fig. 1a). The *ihfA*$^{L-}$ strain produced 1306 mg/L FFAs, 2.07-fold of the Control strain that did not repress the expression of any gene (Fig. 1b). Transcriptomic and proteomic profiles were compared between the *ihfA*$^{L-}$ and Control strains [7]. Hundreds of genes were differentially expressed in the *ihfA*$^{L-}$ strain compared to the Control strain (Fig. S1). Therefore, it is speculated that FFAs overproduction in the *ihfA*$^{L-}$ strain resulted from the comprehensive regulation of cellular processes or physiologies.

To identify beneficial genes facilitating FFAs biosynthesis, down-regulated genes in the *ihfA*$^{L-}$ strain were applied for reverse engineering via CRISPRi. We first assessed the significantly down-regulated genes from comparative transcriptomics of the *ihfA*$^{L-}$ and Control strains ($\log_2$ fold change (FC) < -4). The transcript abundances of these genes are summarized in Fig. S2a. CRISPRi was utilized to repress the expression of 60 selected genes, except those that have been engineered previously [7]. The engineered strains harboring dCas9 and the respective sgRNAs were constructed and cultured. Several strains were unable to grow, which might be due to the perturbation of crucial cellular processes, such as ribosome assembly (Fig. 1c–Table S1). Among the engineered strains, 10 strains obtained a significant increase in FFAs biosynthesis (Fig. 1d). Specifically, the *pspA*^{i}, *rpsK*^{i}, *ompX*^{i}, *dps*^{i}, *iadA*^{i}, *gatY*^{i}, *sodB*^{i}, *sra*^{i}, *rbsB*^{i}, and *gltI*^{i} strains enhanced FFAs production by 93 %, 39 %, 51 %, 36 %, 39 %, 25 %, 43 %, 26 %, 81 %, and 76 %, respectively (Fig. 1d). What's more, the *pspA*^{i} strain produced the highest FFAs titer of 1215 mg/L, 1.93-fold of the Control strain (Fig. 1d). Subsequently, we evaluated the significantly down-regulated genes from comparative proteomics of the *ihfA*$^{L-}$ and Control strains ($\log_2$ FC < -0.86). The abundances of these genes at the protein level are summarized in Fig. S2b. Similarly, CRISPRi was employed to repress the expression of the 17 selected genes, except that have been examined in the above part or our previous study [7]. The engineered strains were constructed and three strains were seriously impaired in cell growth and did not be cultured (Fig. 1e–Table S1). The FFAs assay result demonstrated that reducing the expression of *pspD*, *yhcN*, *yegU*, and *phoA* enhanced FFAs titer by 25 %, 22 %, 72 %, and 22 %, respectively (Fig. 1f). In total, we identified 14 beneficial genes that could enhance FFAs production by repressing their expression. The FFAs titer obtained through repressing each of these genes did not exceed that of the *ihfA*$^{L-}$ strain, showcasing the synergistic function of these genes in FFAs production.

To confirm the down-regulation of the target genes, the engineered strains (*pspA*^{i}, *rpsK*^{i}, *ompX*^{i}, *dps*^{i}, *iadA*^{i}, *gatY*^{i}, *sodB*^{i}, *sra*^{i}, *rbsB*^{i}, *gltI*^{i}, *pspD*^{i}, *yhcN*^{i}, *yegU*^{i}, *phoA*^{i}) and the Control strain were subjected to qRT-PCR analysis. The results showed that the expression levels of the *pspA*, *rpsK*, *ompX*, *dps*, *iadA*, *gatY*, *sodB*, *sra*, *rbsB*, *gltI*, *pspD*, *yhcN*, *yegU*, *phoA* genes in the engineered strains were reduced to 71 %, 81 %, 41 %, 25 %, 34 %, 71 %, 74 %, 21 %, 33 %, 52 %, 59 %, 65 %, 53 %, and 60 % of that in the Control strain, respectively (Fig. S3a). Additionally, we observed that almost all of these 14 engineered strains exhibited higher OD_{600} value and specific FFAs titer (FFAs/OD_{600}) compared to those of the Control strain (Fig. S3b). These results suggest that the repression of these genes improved both cell growth and FFA synthesis, leading to FFAs overproduction in the engineered strains.

3.2. Analysis and classification of beneficial genes

According to gene function, these beneficial targets were classified into three categories, including membrane-related genes, oxidative stress-related genes, and others (Table 1) [32]. *pspA*, *rbsB*, *gltI*, *ompX*, *pspD*, and *phoA* are membrane-related genes. *pspA* and *pspD* belong to the phage shock protein operon, encoding peripheral inner membrane proteins [33,34]. *rbsB* encodes the ribose-binding protein of an ATP-dependent ribose uptake system, and *gltI* encodes the glutamate/aspartate import solute-binding protein, both of which are involved in membrane transport [35]. OmpX is a small outer-membrane protein [36]. Alkaline phosphatase PhoA is secreted across the inner membrane to the periplasmic space and catalyzes the hydrolysis and transphosphorylation of phosphate monoesters. Oxidative stress-related genes include *sodB*, *dps*, and *yhcN*. SodB is one of three superoxide dismutases, implicated in the cellular response to superoxide radicals [37]. Dps is a highly abundant protein in the stationary phase and partakes in protection from oxidative stress. YhcN was also shown to be involved in the response to hydrogen peroxide stress [38]. Five other genes are *yegU*, *iadA*, *rpsK*, *sra*, and *gatY*, encoding putative ADP-ribosylglycohydrolase, isoaspartyl dipeptidase, 30S ribosomal subunit protein S11, 30S ribosomal subunit-associated protein, and tagatose-1,6-bisphosphate aldolase 2, respectively [39–41].

Table 1
The identified genes that enhanced FFAs production via CRISPRi in this study.

Category	Gene	Function	FFAs (mg/L)
Membrane	*pspA*	phage shock protein A	1215
	rbsB	d-ribose ABC transporter periplasmic binding protein	1144
	gltI	glutamate/aspartate periplasmic binding protein	1110
	ompX	outer membrane protein X	953
	pspD	phage shock protein D	787
	phoA	alkaline phosphatase	770
Oxidative stress	*sodB*	superoxide dismutase (Fe)	900
	dps	stationary phase nucleoid protein	856
	yhcN	DUF1471 domain-containing stress-induced protein	767
Others	*yegU*	putative ADP-ribosylglycohydrolase	1087
	iadA	isoaspartyl dipeptidase	877
	rpsK	30S ribosomal subunit protein S11	876
	sra	ribosome-associated protein	792
	gatY	tagatose 1,6-bisphosphate aldolase 2	790

3.3. Membrane characterization

In the above part, we identified that repressing six membrane-related genes contributed to an increased FFAs titer (Table 1). To reveal the association between FFAs overproduction and repression of *pspA*, *rbsB*, *gltI*, *ompX*, *pspD*, and *phoA*, we assessed the membrane properties of the engineered strains (Fig. 2). Membrane lipid of the corresponding strains was determined and presented in terms of membrane lipid distribution and average length of membrane lipid tails. The membrane lipid characterized here is measured by using the Bligh-Dyer method [27,28] and displayed in Fig. 2a. As to the membrane lipid distribution, the proportion of C16 and C18 in the *pspA*^{i}, *rbsB*^{i}, *gltI*^{i}, *ompX*^{i}, *pspD*^{i}, and *phoA*^{i} strains were in the range of 67 %–72 %, higher than that of the Control strain (about 64 %) (Fig. 2b). Likewise, the average lipid length of the *pspA*^{i}, *rbsB*^{i}, *gltI*^{i}, *ompX*^{i}, *pspD*^{i}, and *phoA*^{i} strains increased by 0.21, 0.31, 0.29, 0.20, 0.42, 0.35, respectively, compared to the Control strain (Fig. 2c). In the *ihfA*$^{L-}$ strain, the proportion of C16 and C18 lipid and average lipid length were also higher than those of the Control strain (Fig. 2b and c). We found that all these FFAs-overproducing strains were with increased length of membrane lipid tails compared to the Control strain. We also characterized cell surface hydrophobicity of the recombinant strains by using the microbial adhesion to hydrocarbon (MATH) method. The results showed that the *pspA*^{i}, *pspD*^{i}, *rbsB*^{i}, *gltI*^{i}, *ompX*^{i}, and *phoA*^{i} strains decreased hydrophobicity to 49 %, 62 %, 55 %, 17 %, 53 %, 76 % of that of the Control strain, respectively (Fig. 2d). Besides, the *ihfA*$^{L-}$ strain presented 77 % cell surface hydrophobicity of the Control strain (Fig. 2d). We found that the engineered strains producing higher titer of FFAs have lower cell surface hydrophobicity than the Control strain.

It is well known that the synthesized FFAs could be incorporated into the membrane, regulating membrane composition and properties [42]. As to the synthesized FFAs, the proportion of C16 and C18 species and average fatty acid length in the *pspA*^{i}, *pspD*^{i}, *rbsB*^{i}, *gltI*^{i}, *ompX*^{i}, *phoA*^{i}

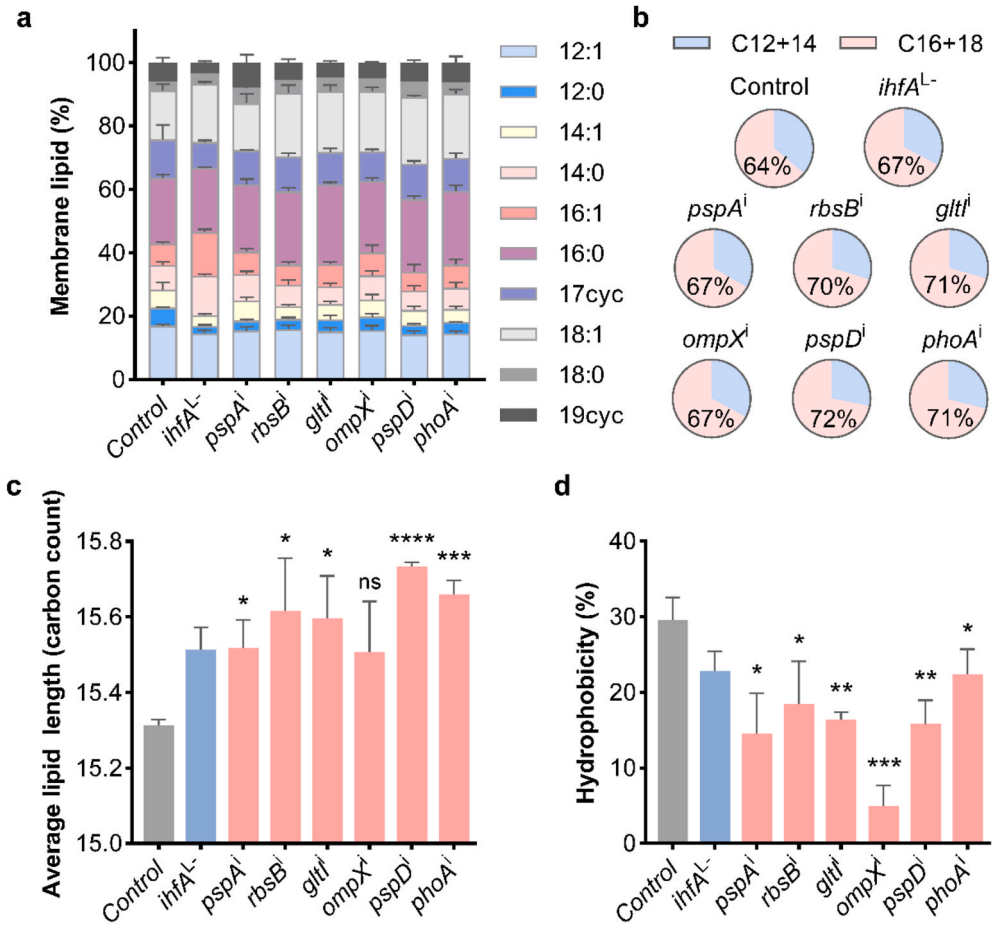

Fig. 2. Membrane characterization of the strains that modulate membrane-related genes. (a) Membrane lipid composition. (b) Membrane lipid distribution. (c) Average length of membrane lipid tails. (d) Hydrophobicity. Error bars on graphs are presented as s.d.

strains was higher than that of the Control strain (Fig. S4). These engineered strains were with increased average length of membrane lipid tails and lower cell surface hydrophobicity than the Control strain (Fig. 2). The increase in average length of membrane lipid tails could augment membrane thickness, enlarge the distance for permeation across the membrane, and thus improve cellular resistance [43], supporting the cellular phenotype of FFAs overproduction (Fig. 3a). Cell surface hydrophobicity was demonstrated to mediate the interaction between membrane and hydrophobic compounds [44,45]. Decreasing cell surface hydrophobicity could weaken the interaction with

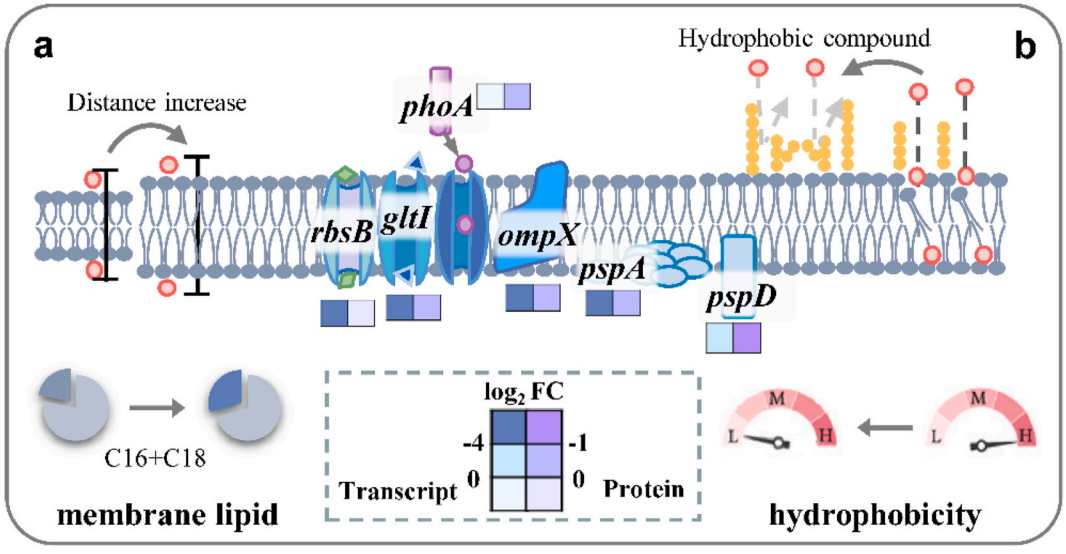

Fig. 3. Mechanistic inference of FFAs overproduction upon modulating membrane-related genes. (a) The enlarged lipid length could increase the distance for permeation across the membrane. (b) The decreased cell surface hydrophobicity could weaken the intercalation of hydrophobic compounds into the membrane.

hydrophobic compounds, prevent its intercalation into the membrane, maintain membrane homeostasis [45], and thus enhance the robustness of industrial strains and contribute to FFAs biosynthesis (Fig. 3b). For improving FFAs production, many efforts have been made to adjustment of microbial membrane functions and biophysical properties through manipulation of membrane biosynthesis pathways and composition [43, 46–48]. Nevertheless, our study identified novel membrane-related targets that have not been engineered for FFAs production, which complements results from previous membrane engineering and advances our understanding of the genes that govern FFAs production.

3.4. ROS determination

In the above part, we also identified that repressing three oxidative stress-related genes contributed to an increased FFAs titer (Table 1). To reveal the association between FFAs overproduction and repression of *sodB*, *dps*, and *yhcN*, we assessed the ROS level of the engineered strains, which are highly reactive molecules leading to oxidative stress [49]. ROS was characterized using a microplate reader and fluorescence microscopy, based on the oxidation of dichlorofluorescin (DCFH) to dichlorofluorescein (DCF). The results showed that the dps^{i}, $sodB^{i}$, and $yhcN^{i}$ strains presented a decreased fluorescence of 63 %, 38 %, and 46 %, respectively, compared with the Control strain (Fig. 4a). Likewise, ROS in the $ihfA^{L-}$ strain decreased to 64 % of that in the Control strain (Fig. 4a). As consistent with fluorescence microscopy image, only a residual fluorescent signal was detected in the engineered strains and the $ihfA^{L-}$ strain, while a strong signal derived from DCF fluorescent probe was measured in the Control strain (Fig. 4b–f).

The engineered strains dps^{i}, $sodB^{i}$, and $yhcN^{i}$ producing high titer of FFAs did not exacerbate the generation of ROS (Fig. 4). SodB, Dps, and YhcN were demonstrated to function as ROS detoxification. However, it was observed that overexpression of *dps*, *yhcN*, or *sodB* contrarily increased ROS levels (Fig. S5). Indeed, overproduction of proteins has been shown to induce oxidative stress responses and lead to ROS generation [50,51]. Therefore, the expression of this kind of protein is presumed to be unwanted or unnecessary at low ROS levels [37,52]. We speculate that reducing the expression of *sodB*, *dps*, and *yhcN* will save resources of energy and substrates in the process of transcription and translation for the biosynthesis of FFAs (Fig. 5). Our results point out an important note that cellular response to stress needs to be modulated appropriately rather than blindly reinforced, although they are seemingly beneficial cellular processes when cells are under stress.

4. Conclusion

In this study, we identify the role of the global regulator IhfA for FFAs overproduction using CRISPRi-facilitated reverse engineering and cellular physiological characterization. Firstly, a total of 14 beneficial genes that could enhance FFAs production were identified via CRISPRi from the differentially expressed genes in the $ihfA^{L-}$ strain. Then, the functions of beneficial genes were analyzed and determined. Repression of *pspA*, *rbsB*, *gltI*, *ompX*, *pspD*, and *phoA* could increase the average

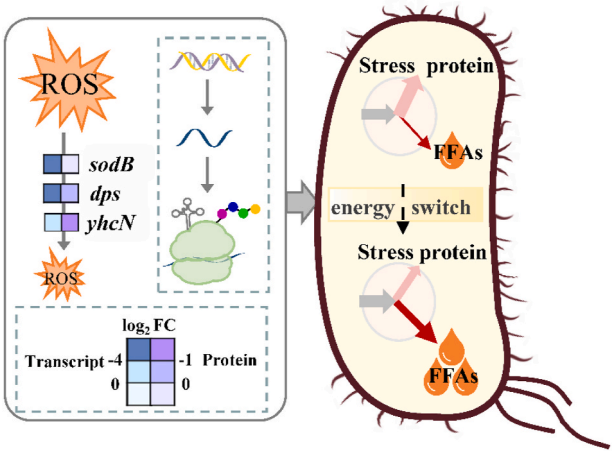

Fig. 5. Mechanistic inference of FFAs overproduction upon modulating genes related to oxidative stress. Reducing the expression of *sodB*, *dps*, and *yhcN* could save cell resources in the process of transcription and translation for the biosynthesis of FFAs.

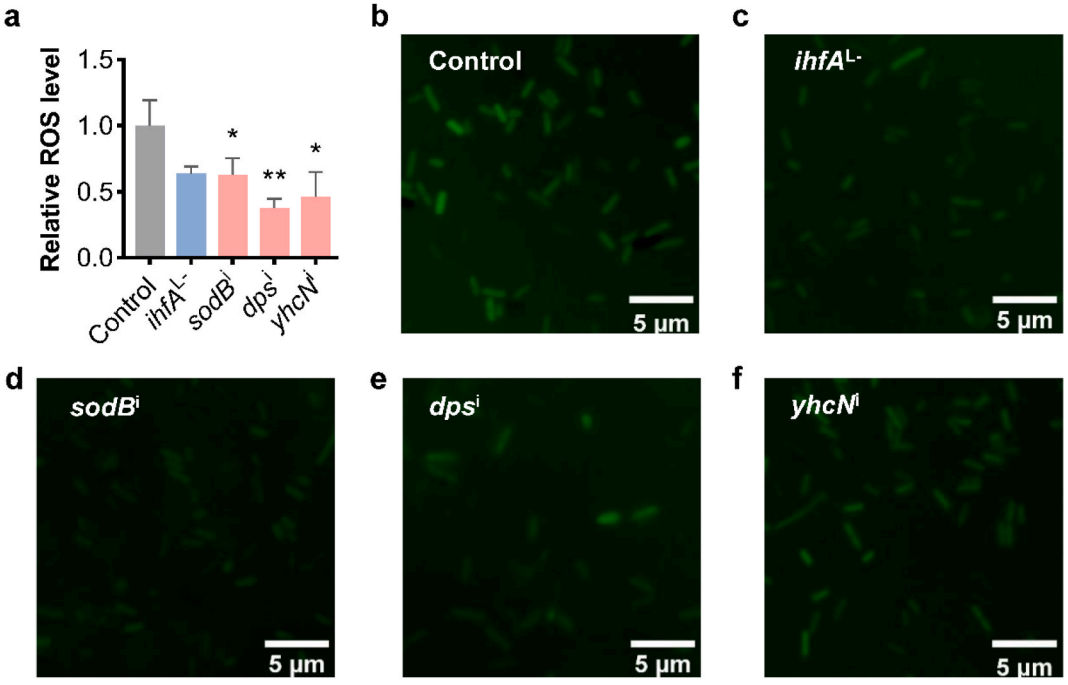

Fig. 4. ROS level of the strains modulating genes related to oxidative stress. (a) Relative ROS level detected by a microplate reader. Error bars on graphs are presented as s.d. (b–f) ROS fluorescence intensity in the Control, $ihfA^{L-}$, $sodB^{i}$, dps^{i}, or $yhcN^{i}$ strain detected by fluorescence microscopy.

length of membrane lipid tails and decrease cell surface hydrophobicity, contributing to the enhancement of cellular robustness and FFAs biosynthesis. Repression of *sodB*, *dps*, and *yhcN* could reduce the ROS level and might save wasteful consumption of cellular resources, making cells robust and well-prepared for FFAs production. Collectively, our findings shed light on the association between FFAs biosynthesis with membrane and oxidative regulation, aiding in further improvement in FFAs bioproduction.

CRediT authorship contribution statement

Lixia Fang: conceived and designed the experiments, Writing – original draft. **Ziyi Han:** performed the plasmids construction, tube fermentation, qRT-PCR analysis, ROS measurement, Writing – original draft. **Xueru Feng:** performed the plasmids construction and tube fermentation. **Xueyan Hao:** membrane characterization. **Mengxiao Liu:** ROS measurement. **Hao Song:** revised the manuscript. **Yingxiu Cao:** conceived and designed the experiments, revised the manuscript, supervised the study. All authors contributed to the article and approved the submitted version.

Declaration of competing interest

The authors declare that they have no known competing financial interests or personal relationships that could have appeared to influence the work reported in this paper.

Acknowledgements

This work was supported by the National Key Research and Development Program of China (2021YFC2104400), the National Natural Science Foundation of China (NSFC 22078240), and the China Postdoctoral Science Foundation (2022M722359).

Appendix A. Supplementary data

Supplementary data to this article can be found online at https://doi.org/10.1016/j.synbio.2024.01.007.

References

[1] Liu Y, Benitez MG, Chen J, Harrison E, Khusnutdinova AN, Mahadevan R. Opportunities and Challenges for microbial synthesis of fatty acid-derived chemicals (FACs). Front Bioeng Biotechnol 2021;9:613322. https://doi.org/10.3389/fbioe.2021.613322.

[2] Yan Q, Pfleger BF. Revisiting metabolic engineering strategies for microbial synthesis of oleochemicals. Metab Eng 2020;58:35–46. https://doi.org/10.1016/j.ymben.2019.04.009.

[3] Chen X, Gao C, Guo L, Hu G, Luo Q, Liu J, Nielsen J, Chen J, Liu L. DCEO Biotechnology: tools to design, construct, evaluate, and optimize the metabolic pathway for biosynthesis of chemicals. Chem Rev 2018;118(1):4–72. https://doi.org/10.1021/acs.chemrev.6b00804.

[4] Chen Y, Banerjee D, Mukhopadhyay A, Petzold CJ. Systems and synthetic biology tools for advanced bioproduction hosts. Curr Opin Biotechnol 2020;64:101–9. https://doi.org/10.1016/j.copbio.2019.12.007.

[5] Nielsen J. It is all about metabolic fluxes. J Bacteriol 2003;185(24):7031–5. https://doi.org/10.1128/JB.185.24.7031-7035.2003.

[6] Nielsen J, Keasling JD. Engineering cellular metabolism. Cell 2016;164(6):1185–97. https://doi.org/10.1016/j.cell.2016.02.004.

[7] Fang L, Fan J, Luo S, Chen Y, Wang C, Cao Y, Song H. Genome-scale target identification in *Escherichia coli* for high-titer production of free fatty acids. Nat Commun 2021;12(1):4976. https://doi.org/10.1038/s41467-021-25243-w.

[8] Park WS, Shin KS, Jung HW, Lee Y, Sathesh-Prabu C, Lee SK. Combinatorial metabolic engineering strategies for the enhanced production of free fatty acids in *Escherichia coli*. J Agric Food Chem 2022;70(43):13913–21. https://doi.org/10.1021/acs.jafc.2c04621.

[9] Xu P, Gu Q, Wang W, Wong L, Bower AG, Collins CH, Koffas MA. Modular optimization of multi-gene pathways for fatty acids production in *E. coli*. Nat Commun 2013;4:1409. https://doi.org/10.1038/ncomms2425.

[10] Marella ER, Holkenbrink C, Siewers V, Borodina I. Engineering microbial fatty acid metabolism for biofuels and biochemicals. Curr Opin Biotechnol 2018;50:39–46. https://doi.org/10.1016/j.copbio.2017.10.002.

[11] Deng C, Wu Y, Lv X, Li J, Liu Y, Du G, Chen J, Liu L. Refactoring transcription factors for metabolic engineering. Biotechnol Adv 2022;57:107935. https://doi.org/10.1016/j.biotechadv.2022.107935.

[12] Fujita Y, Matsuoka H, Hirooka K. Regulation of fatty acid metabolism in bacteria. Mol Microbiol 2007;66(4):829–39. https://doi.org/10.1111/j.1365-2958.2007.05947.x.

[13] Zhu K, Zhang YM, Rock CO. Transcriptional regulation of membrane lipid homeostasis in *Escherichia coli*. J Biol Chem 2009;284(50):34880–8. https://doi.org/10.1074/jbc.M109.068239.

[14] Wang D, Thakker C, Liu P, Bennett GN, San KY. Efficient production of free fatty acids from soybean meal carbohydrates. Biotechnol Bioeng 2015;112(11):2324–33. https://doi.org/10.1002/bit.25633.

[15] Zhang F, Carothers JM, Keasling JD. Design of a dynamic sensor-regulator system for production of chemicals and fuels derived from fatty acids. Nat Biotechnol 2012;30(4):354–9. https://doi.org/10.1038/nbt.2149.

[16] Mumm JP, Landy A, Gelles J. Viewing single lambda site-specific recombination events from start to finish. EMBO J 2006;25(19):4586–95. https://doi.org/10.1038/sj.emboj.7601325.

[17] Dorman CJ. Function of nucleoid-associated proteins in chromosome structuring and transcriptional regulation. J Mol Microbiol Biotechnol 2014;24(5–6):316–31. https://doi.org/10.1159/000368850.

[18] Kyle Bennett R, Agee A, Har JRG, von Hagel B, Antoniewicz MR, Papoutsakis ET. Regulatory interventions improve the biosynthesis of limiting amino acids from methanol carbon to improve synthetic methylotrophy in *Escherichia coli*. Biotechnol Bioeng 2021;118(1):43–57. https://doi.org/10.1002/bit.27549.

[19] Larson MH, Gilbert LA, Wang X, Lim WA, Weissman JS, Qi LS. CRISPR interference (CRISPRi) for sequence-specific control of gene expression. Nat Protoc 2013;8(11):2180–96. https://doi.org/10.1038/nprot.2013.132.

[20] Ghavami S, Pandi A. CRISPR interference and its applications. Prog Mol Biol Transl Sci 2021;180:123–40. https://doi.org/10.1016/bs.pmbts.2021.01.007.

[21] Zhang R, Xu W, Shao S, Wang Q. Gene silencing through CRISPR interference in bacteria: Current advances and Future Prospects. Front Microbiol 2021;12:635227. https://doi.org/10.3389/fmicb.2021.635227.

[22] Concordet JP, Haeussler M. CRISPOR: intuitive guide selection for CRISPR/Cas9 genome editing experiments and screens. Nucleic Acids Res 2018;46(W1):W242–5. https://doi.org/10.1093/nar/gky354.

[23] Bikard D, Jiang W, Samai P, Hochschild A, Zhang F, Marraffini LA. Programmable repression and activation of bacterial gene expression using an engineered CRISPR-Cas system. Nucleic Acids Res 2013;41(15):7429–37. https://doi.org/10.1093/nar/gkt520.

[24] Engler C, Kandzia R, Marillonnet S. A one pot, one step, precision cloning method with high throughput capability. PLoS One 2008;3(11):e3647. https://doi.org/10.1371/journal.pone.0003647.

[25] Cao YX, Xiao WH, Zhang JL, Xie ZX, Ding MZ, Yuan YJ. Heterologous biosynthesis and manipulation of alkanes in *Escherichia coli*. Metab Eng 2016;38:19–28. https://doi.org/10.1016/j.ymben.2016.06.002.

[26] Zhang F, Ouellet M, Batth TS, Adams PD, Petzold CJ, Mukhopadhyay A, Keasling JD. Enhancing fatty acid production by the expression of the regulatory transcription factor FadR. Metab Eng 2012;14(6):653–60. https://doi.org/10.1016/j.ymben.2012.08.009.

[27] Bligh EG, Dyer WJ. A rapid method of total lipid extraction and purification. Can J Biochem Physiol 1959;37(8):911–7. https://doi.org/10.1139/o59-099.

[28] Chen Y, Reinhardt M, Neris N, Kerns L, Mansell TJ, Jarboe LR. Lessons in membrane engineering for Octanoic acid production from environmental *Escherichia coli* Isolates. Appl Environ Microbiol 2018;84(19). https://doi.org/10.1128/AEM.01285-18.

[29] Rosenberg M. Microbial adhesion to hydrocarbons: twenty-five years of doing MATH. FEMS Microbiol Lett 2006;262(2):129–34. https://doi.org/10.1111/j.1574-6968.2006.00291.x.

[30] Sun T, Pei G, Wang J, Chen L, Zhang W. A novel small RNA CoaR regulates coenzyme A biosynthesis and tolerance of *Synechocystis* sp. PCC6803 to 1-butanol possibly via promoter-directed transcriptional silencing. Biotechnol Biofuels 2017;10:42. https://doi.org/10.1186/s13068-017-0727-y.

[31] Sun T, Li S, Song X, Pei G, Diao J, Cui J, Shi M, Chen L, Zhang W. Re-direction of carbon flux to key precursor malonyl-CoA via artificial small RNAs in photosynthetic *Synechocystis* sp. PCC 6803. Biotechnol Biofuels 2018;11:26. https://doi.org/10.1186/s13068-018-1032-0.

[32] Karp PD, Ong WK, Paley S, Billington R, Caspi R, Fulcher C, Kothari A, Krummenacker M, Latendresse M, Midford PE, Subhraveti P, Gama-Castro S, Muniz-Rascado L, Bonavides-Martinez C, Santos-Zavaleta A, Mackie A, Collado-Vides J, Keseler IM, Paulsen I. The EcoCyc database. EcoSal Plus 2018;8(1). https://doi.org/10.1128/ecosalplus.ESP-0006-2018.

[33] Bergler H, Abraham D, Aschauer H, Turnowsky F. Inhibition of lipid biosynthesis induces the expression of the *pspA* gene. Microbiology (Reading, England) 1994;140(Pt 8):1937–44. https://doi.org/10.1099/13500872-140-8-1937.

[34] Brissette JL, Weiner L, Ripmaster TL, Model P. Characterization and sequence of the *Escherichia coli* stress-induced *psp* operon. Journal of molecular biology 1991;220(1):35–48. https://doi.org/10.1016/0022-2836(91)90379-k.

[35] Clifton MC, Simon MJ, Erramilli SK, Zhang H, Zaitseva J, Hermodson MA, Stauffacher CV. In vitro reassembly of the ribose ATP-binding cassette transporter reveals a distinct set of transport complexes. J Biol Chem 2015;290(9):5555–65. https://doi.org/10.1074/jbc.M114.621573.

[36] Dupont M, James CE, Chevalier J, Pagès JM. An early response to environmental stress involves regulation of OmpX and OmpF, two enterobacterial outer membrane pore-forming proteins. Antimicrob Agents Chemother 2007;51(9):3190–8. https://doi.org/10.1128/aac.01481-06.

[37] Doukyu N, Taguchi K. Involvement of catalase and superoxide dismutase in hydrophobic organic solvent tolerance of *Escherichia coli*. Amb Express 2021;11(1):97. https://doi.org/10.1186/s13568-021-01258-w.
[38] Kannan G, Wilks JC, Fitzgerald DM, Jones BD, Bondurant SS, Slonczewski JL. Rapid acid treatment of *Escherichia coli*: transcriptomic response and recovery. BMC Microbiol 2008;8:37. https://doi.org/10.1186/1471-2180-8-37.
[39] Marti-Arbona R, Fresquet V, Thoden JB, Davis ML, Holden HM, Raushel FM. Mechanism of the reaction catalyzed by isoaspartyl dipeptidase from *Escherichia coli*. Biochemistry 2005;44(19):7115–24. https://doi.org/10.1021/bi050008r.
[40] Yu L, Liu X, Yu X. ADP-ribosylhydrolases: from DNA damage repair to COVID-19. J Zhejiang Univ - Sci B 2021;22(1):21–30. https://doi.org/10.1631/jzus.B2000319.
[41] Bheemireddy S, Sandhya S, Srinivasan N. Comparative analysis of structural and dynamical features of ribosome upon association with mRNA reveals potential role of ribosomal proteins. Front Mol Biosci 2021;8:654164. https://doi.org/10.3389/fmolb.2021.654164.
[42] Jackowski S, Jackson PD, Rock CO. Sequence and function of the aas gene in *Escherichia coli*. J Biol Chem 1994;269(4):2921–8.
[43] Tan Z, Khakbaz P, Chen Y, Lombardo J, Yoon JM, Shanks JV, Klauda JB, Jarboe LR. Engineering *Escherichia coli* membrane phospholipid head distribution improves tolerance and production of biorenewables. Metab Eng 2017;44:1–12. https://doi.org/10.1016/j.ymben.2017.08.006.
[44] Liao C, Liang X, Soupir ML, Jarboe LR. Cellular, particle and environmental parameters influencing attachment in surface waters: a review. J Appl Microbiol 2015;119(2):315–30. https://doi.org/10.1111/jam.12860.
[45] Claus S, Jezierska S, Van Bogaert INA. Protein-facilitated transport of hydrophobic molecules across the yeast plasma membrane. FEBS Lett 2019;593(13):1508–27. https://doi.org/10.1002/1873-3468.13469.
[46] Shin KS, Lee SK. Increasing extracellular free fatty acid production in *Escherichia coli* by disrupting membrane transport systems. J Agric Food Chem 2017;65(51):11243–50. https://doi.org/10.1021/acs.jafc.7b04521.
[47] Tan Z, Yoon JM, Nielsen DR, Shanks JV, Jarboe LR. Membrane engineering via trans unsaturated fatty acids production improves *Escherichia coli* robustness and production of biorenewables. Metab Eng 2016;35:105–13. https://doi.org/10.1016/j.ymben.2016.02.004.
[48] Tan Z, Black W, Yoon JM, Shanks JV, Jarboe LR. Improving *Escherichia coli* membrane integrity and fatty acid production by expression tuning of FadL and OmpF. Microb Cell Fact 2017;16(1):38. https://doi.org/10.1186/s12934-017-0650-8.
[49] Avery SV. Molecular targets of oxidative stress. Biochem J 2011;434(2):201–10. https://doi.org/10.1042/BJ20101695.
[50] Malhotra JD, Miao H, Zhang K, Wolfson A, Pennathur S, Pipe SW, Kaufman RJ. Antioxidants reduce endoplasmic reticulum stress and improve protein secretion. Proc Natl Acad Sci U S A 2008;105(47):18525–30. https://doi.org/10.1073/pnas.0809677105.
[51] Huang M, Bao J, Hallstrom BM, Petranovic D, Nielsen J. Efficient protein production by yeast requires global tuning of metabolism. Nat Commun 2017;8(1):1131. https://doi.org/10.1038/s41467-017-00999-2.
[52] Loffler M, Simen JD, Jager G, Schaferhoff K, Freund A, Takors R. Engineering *E. coli* for large-scale production - strategies considering ATP expenses and transcriptional responses. Metab Eng 2016;38:73–85. https://doi.org/10.1016/j.ymben.2016.06.008.